ACS APPLIED MATERIALS & INTERFACES

Research Article

www.acsami.org

High-Strength Nanocellulose–Talc Hybrid Barrier Films

Henrikki Liimatainen,*[,†] Ngesa Ezekiel,[‡] Rafal Sliz,[§] Katja Ohenoja,[†] Juho Antti Sirviö,[∥] Lars Berglund,[‡,⊥] Osmo Hormi,[∥] and Jouko Niinimäki[†]

[†]Fiber and Particle Engineering Laboratory, University of Oulu, P.O. Box 4300, FI-90014, Oulu, Finland

[‡]Fiber and Polymer Technology, Royal Institute of Technology, SE-10044 Stockholm, Sweden

[§]Optoelectronics and Measurement Techniques Laboratory, Department of Electrical Engineering, University of Oulu, FI-90014, Oulu, Finland

[∥]Department of Chemistry, University of Oulu, P.O. Box 3000, FI-90014, Oulu, Finland

[⊥]Department of Fiber and Polymer Technology, Wallenberg Wood Science Center, Royal Institute of Technology, SE-10044 Stockholm, Sweden

Supporting Information

ABSTRACT: Hybrid organic–inorganic films mimicking natural nacre-like composite structures were fabricated from cellulose nanofibers obtained from sequential periodate–chlorite oxidation treatment and talc platelets, using a simple vacuum-filtration method. As a pretreatment, commercial talc aggregates were individualized into well-dispersed talc platelets using a wet stirred media mill with high-shear conditions to promote the homogeneity and mechanical characteristics of hybrids. The nanofiber–talc hybrids, which had talc contents from 1 to 50 wt %, were all flexible in bending, and possessed tensile strength and Young's modulus values up to 211 ± 3 MPa and 12 ± 1 GPa, respectively, the values being remarkably higher than those reported previously for nanofibrillated cellulose–talc films. Because of the lamellar and well-organized structure of hybrids in which the talc platelets were evenly embedded, they possessed a small pore size and good oxygen barrier properties, as indicated by the preliminary results. The talc platelets decreased the moisture adsorption of highly talc-loaded hybrids, although they still exhibited hydrophilic surface characteristics in terms of contact angles.

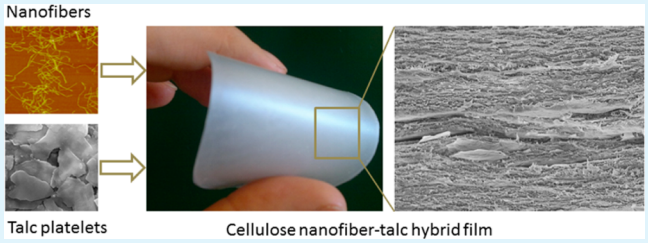

KEYWORDS: *nanocomposite, nanofibrillated cellulose, nanopaper, mineral, talc*

INTRODUCTION

Organic–inorganic hybrid materials mimicking natural composites, such as bone and nacre, have attracted attention during recent years because of their superior mechanical performance.[1,2] In these hybrids, a high content of mineral platelets were incorporated into a polymeric matrix, resulting in lamellar nacre-like, "brick-and-mortar" structures.[3] One high-potential green material that can be used to construct these multifunctional hybrids is nanofibrillar cellulose (NFC), which has a natural tendency to form strong and porous networks, in which the inorganic particles can be homogeneously embedded.[4] The NFC-based hybrids are highly promising, e.g., for light-weight packaging, coatings, and films.[5,6] Moreover, potentially high-performing materials (e.g., for flexible electronics and separation membranes) can possibly be obtained by tailoring NFC hybrid structures.[7−9]

So far, multifunctional NFC-based hybrid materials have been manufactured using montmorillonite platelets in particular,[10−12] but also titanium dioxide (TiO_2),[13] and other layered silicates, such as vermiculite[5,14,15] and mica.[14,15] These nanostructured hybrid structures can be extremely stiff and strong, demonstrating tensile strength and Young's modulus up to 500 MPa and 18 GPa, respectively.[10] Because of the stratified structure of hybrids, in which mineral platelets are organized parallel to the surface, they also hinder gas diffusion, resulting in good oxygen barrier and fire-retardant properties.[16]

Talc is one attractive inorganic material for novel organic–inorganic hybrid structures. It is a lamellar hydrous, magnesium silicate mineral that consists of a three-layer structure in which magnesium oxide is layered between hydrophobic silica layers. Talc has widely been used as a bulk ingredient, e.g., in plastic and papermaking industries.[17] However, there are few reports of talc use in NFC-based materials. Previously, cationic NFC–talc films were manufactured using filtration and hot-pressing methods,[15] but the mechanical properties of talc hybrids were significantly lower than those of others, e.g., montmorillonite (e.g., tensile strength of 67 ± 13 vs 116 ± 5 MPa, respectively). This drawback was probably due to talc platelet aggregation and large aggregate size (> 10 μm).[14] A homogenization process was used to decrease the degree of aggregation, but the

Received: October 2, 2013
Accepted: November 11, 2013
Published: November 11, 2013

applied conditions were probably not intensive enough to break down the aggregates. Consequently, enhanced mechanical properties are expected from the use of well-dispersed individual platelets, instead of aggregates. The NFC−talc hybrids may also possess special characteristics, compared to those of other minerals, because of the hydrophobic nature and softness of talc platelets. These properties may improve the characteristics of hybrids in high-humidity conditions, since the structural swelling caused by the hydrophilicity of NFCs and layered silicates other than talc has been found to increase network porosity.[12,18]

Therefore, in this study, we aimed to prepare high-strength NFC hybrid films with a vacuum-filtration method using individual talc platelets instead of previously used talc aggregates. The talc platelets were individualized from commercial talc aggregates using wet stirred media milling with high-shear conditions. To optimize the mechanical properties of hybrids, well-dispersed and chemically modified cellulose nanofibers having a dicarboxylic acid functionality and a width of 3−20 nm were prepared using sequential periodate−chlorite oxidation.[19] The anionic surface charge density of nanofibers was assumed to decrease nanofiber aggregation during film preparation and to enable formation of a homogenous and continuous network in which the individual talc platelets can be tightly embedded to form a nacre-like lamellar structure. The structural, mechanical, surface chemical (wetting), optical, and barrier properties of hybrid films were characterized using atomic force microscopy (AFM), field emission scanning electron microscopy (FESEM), tensile testing, contact angle measurement, ultraviolet−visible light (UV−vis) spectroscopy, and oxygen permeability analysis.

EXPERIMENTAL SECTION

Materials. Sequential periodate−chlorite oxidation pretreatment (the reaction route is shown in Figure S1 in the Supporting Information), combined with high-pressure homogenization, was employed to produce dicarboxylic acid cellulose nanofibers (DCC) from bleached birch (*Betula pendula*) chemical wood pulp, according to a previously described method.[19] In brief, a sample of disintegrated cellulose pulp (6 g dry weight) was allowed to react for 2 h with sodium metaperiodate ($NaIO_4$) in deionized water (total volume of 600 mL) at 55 °C to obtain dialdehyde cellulose. The sample was subsequently filtered, washed, and further reacted with sodium chlorite ($NaClO_2$) in a 1 M aqueous solution of acetic acid for 48 h at room temperature to obtain dicarboxylic acid cellulose. The oxidized product (aldehyde content of 1.31 ± 0.12 mmol/g) was filtered and washed with deionized water until the conductivity of the filtrate was <10 μS/cm. The carboxyl content of oxidized pulp was 1.20 ± 0.05 mmol/g, as determined using a conductometric titration.[20,21] The suspension containing 0.5% (w/w) of oxidized cellulose fibers at a pH of approximately 7 was nanofibrillated using a two-chamber high-pressure homogenizer (APV-2000, Denmark) with a pressure of 400−950 bar. The suspension was passed through the homogenizer three times until a clear, DCC nanofiber-containing gel was obtained. All of the chemicals used in the periodate and chlorite oxidations ($NaIO_4$, $NaClO_2$, and CH_3COOH) and carboxyl content analyses (NaCl and NaOH) were obtained as p.a. grade from Sigma-Aldrich (Germany) without further purification.

Talc was obtained from IMI FABI SpA (Italy) in the form of a dry powder with a particle size of 20 μm, as measured by a laser diffraction technique (Beckman Coulter LS 13 320, Mie optical model, USA). The talc's particle size was further reduced by laboratory-scale grinding using a stirred media mill (Hosokawa Alpine 90 AHM hydro mill, Germany), which was operated in circuit mode for 11 h. Yttria-stabilized zirconium oxide beads with a size of 1 mm were used as the grinding media, and a stirrer tip speed of 11 m/s was used. The volumetric mean particle size of the ground talc, as obtained with a laser diffraction technique (Beckman Coulter LS 13 320, USA), was 1.14 μm. The surface charge density, measured with polyelectrolyte titration (Mütek PCD 03, USA), was 44 μeq/g. A 0.5 wt % talc particle dispersion was prepared in deionized water for the DCC−talc hybrid film preparation, using an UltraTurrax mixer (Germany) at 10 000 rpm for 5 min.

Preparation of DCC−Talc Hybrid Films. A vacuum-filtration method was used to prepare DCC nanofiber−talc hybrid films.[11,22] The DCC nanofiber and talc dispersions (total solids of 150 mg in 200 g of deionized water) were mixed together using an UltraTurrax mixer at 10 000 rpm for 10 min and degassed under a vacuum for 24 h. The suspensions with DCC/talc weight ratios of 100:0, 99:1, 90:10, 75:25, and 50:50 (coded as DCC100, DCC99-Talc1, DCC90-Talc10, DCC75-Talc25, and DCC50-Talc50, respectively) were vacuum-filtered on a filter membrane with a pore size of 0.65 μm (Millipore, USA), after which the wet film was vacuum-dried between metal cloths by a Rapid Köthen equipment (Germany) at 94 °C for 10 min.

Atomic Force Microscopy. An AFM (Nanoscope IIIA, Veeco Instruments, Santa Barbara, CA USA) was performed to reveal the morphology of DCC nanofibers. As a pretreatment, the nanofiber suspension of 0.001% was sonicated for 1 min to enable complete disentanglement and dispersion of nanofibers. A fresh mica surface, which was pretreated with cationic polyelectrolyte (polylysine, Sigma-Aldrich, Germany), was used as a substrate for nanofibers. The dilute DCC nanofiber suspension was cast on the pretreated mica surface and air-dried. The AFM images were captured in a tapping mode using a 8 nm steel tip.

Field Emission Scanning Electron Microscopy. An FESEM (Zeiss Ultra Plus, Germany and JOEL S-4800, Hitachi, Japan) was employed to study the structural properties of talc platelets and DCC−talc hybrid films in planar and cross-sectional directions. Prior to FESEM imaging, the DCC−talc samples were conditioned overnight in a desiccator to remove moisture and then coated with gold/palladium using the SEM sputter coater to improve the sample's electric conductivity. The images of the structure were captured from the secondary electrons released from the sample's surface after bombardment with a beam of electrons accelerated at 1.0 kV. The ground talc sample was first diluted with deionized water to 0.01 wt %; after that, a droplet of sample was dried in the oven (26 °C). The dried sample was sputter-coated with platinum. An electron voltage of 10 kV and a working distance of 5 mm were used for imaging.

Light Transmittance. The light transmittance of DCC−talc hybrid films at 550 nm was measured with a Hach DR 2800 spectrophotometer (USA).

Tensile Test. The mechanical properties of the films were measured with a universal materials testing machine (Instron 5944, U.K.), using a 500 N load cell. The measurements were conducted at 50% humidity and 20 °C temperature, using specimens of 40 mm in length, approximately 40 μm in thickness, and 5 mm in width with a strain rate of 4 mm/min. The samples were conditioned in a measuring environment for 48 h before testing. At least five replicates were measured for each sample.

Density and Porosity Measurement. A gas pycnometer (AccuPyc II 1340 Micromeritics, USA), based on helium gas displacement, was used to measure the true density (ρ_t) and volume (V_t) of DCC−talc hybrid films. The pycnometer measures the true volume of the sample (i.e., it excludes open pores of the sample), from which the true density can be calculated using the sample weight.[23] The porosity of the sample (Φ) was determined as the ratio of true volume and bulk volume (V_b) determined by a micrometer, according to eq 1:

$$\Phi = (V_t/V_b)*100\% \quad (1)$$

Contact Angle Measurement. Surface interactions between DCC−talc hybrid films and deionized water were investigated by applying the static sessile-drop, contact angle measurement method at room temperature. The measurements were performed immediately after the formation of drops on the film surface, using a Krüss DSA100 (Germany) system. The instrument was equipped with a high-speed

camera (360 fps) and analysis software. Contact angles were extracted using the height−width method, in which a contour line enclosed by a rectangle is regarded as a segment of a circle. As a result, the contact angle can be calculated from the height−width relationship of the enclosing rectangle. For each sample, surface contact angles of droplets at three different locations were averaged out, and standard deviations were calculated.

Moisture Adsorption Test. Moisture adsorption of DCC−talc hybrid films was measured at 80% humidity and 20 °C temperature by weighing samples until a constant weight was obtained. The samples were dried at 60 °C for 24 h before measurements.

Oxygen Transmission Rate. The oxygen transmission rate (OTR) of DCC−talc films was measured at 50% humidity and 23 °C temperature using a Mocon OX-Tran Twin (USA) instrument.

RESULTS AND DISCUSSION

Structural Characteristics of Hybrids. A simple vacuum-filtration technique, followed by vacuum drying,[11,22] was used to fabricate self-standing NFC−talc hybrid films from dicarboxylic acid cellulose nanofibers and individual talc platelets. Typical lateral dimensions of DCC nanofibers ranged from 3 to 5 nm, as determined by AFM (Figure 1A), while their length was up to micrometer scale. The nanofiber suspension contained also shorter fibers, which can originate from cutting of longer nanofibrils due to oxidative pretreatment. The NFC suspension was used directly after the preparation with a homogenizer without any purification steps, and consequently, it also contained some larger fibril bundles of diameters below 200 nm. Because of the small size and relatively high charge density of nanofibers (1.20 meq/g), which reduced flocculation between NFCs, the suspension existed in the form of a transparent and stable gel. The visual appearance of the NFC gel and oxidized cellulose is presented in Figure S2 in the Supporting Information.

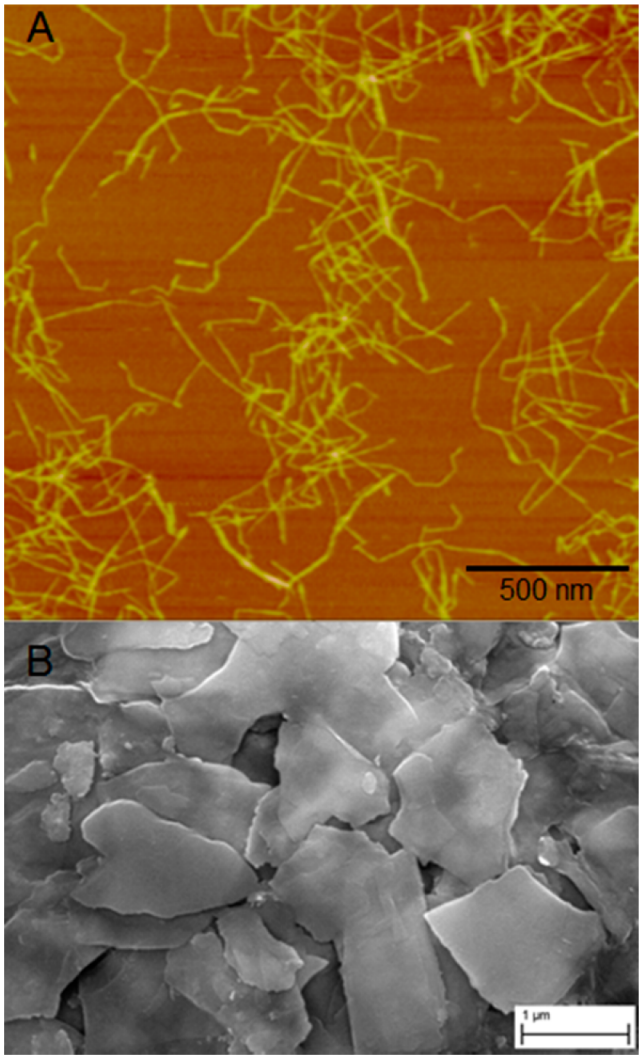

Figure 1. (A) AFM micrograph of dicarboxylic acid cellulose (DCC) nanofibers. (B) FESEM image of talc platelets.

Talc platelets, which were obtained using wet stirred media milling, had an average particle size of 1.14 μm, as determined using a laser diffraction technique. This result reflects the size of the longest dimension of platelets[24] and shows that the particle size of talc was significantly reduced from the original 20 μm. According to FESEM imaging (Figure 1B), the sample contained individual platelets without aggregates, which were approximately 20 nm in thickness and had a planar length scale from a few hundreds of nanometers to over a micrometer, and a corresponding aspect ratio from 20 to 60. The size of talc particles was significantly smaller than those of previously reported NFC−talc hybrids.[14]

High-shear mixing was used to improve the homogeneity of the mixed DCC nanofiber−talc platelet suspension before film fabrication. The suspension, which had a visual appearance from transparent to highly turbid, depending on the talc content used, was immediately filtered after mixing to avoid aggregation of constituents and sedimentation of possible bigger flocs. However, from visual observation, no flocculation was apparent between DCC and talc particles during filtration. It is likely that the anionic charge of both DCC and talc platelets prevented aggregation between constituents and promoted the stability of the suspension.

Figure 2 shows the morphology of fabricated DCC−talc hybrid films in planar and cross-sectional directions, obtained using FESEM. The surfaces of DCC99-Talc1 and DCC90-Talc10 exhibited a highly homogeneous, smooth, and dense structure, but also contained some larger nanofibril aggregates, which may have originated from poorly fibrillated fibers. From a top-down view, DCC75-Talc25 and DCC50-Talc50 hybrids, in turn, contained clearly visible talc platelets, which were connected by DCC nanofibers. The surfaces of these samples seemed to be rougher and more nonhomogeneous than those of films with lower talc content. Cross-sectional images of all hybrids clearly presented their layered structure, which resembled the brick-and-mortar structure of natural nacre-like composites.[25] Talc platelets were evenly distributed in cross section and aligned parallelly to the hybrid surface. This microscale architecture was similar to a "sheet nacre" structure, which has platelets ordered randomly in lamellar layers.[3] Contrary to previous results of cationic NFC and talc hybrids,[15] talc aggregation was not detected in the present cross-sectional views.

Similar to nacre structures, the hybrid films contained also pores in nanoscale. The amount of interconnecting pores of lamellae (pores can be seen as black areas in the FESEM images), which had a size below 50 nm, appears to decrease as a function of talc content. This result proved that talc platelets effectively sealed the voids of a porous nanofiber network and suggested that talc platelets were strongly incorporated into the structure, despite the fact that both nanofibers and talc were anionically charged. As earlier stated,[14] the repulsive electro-

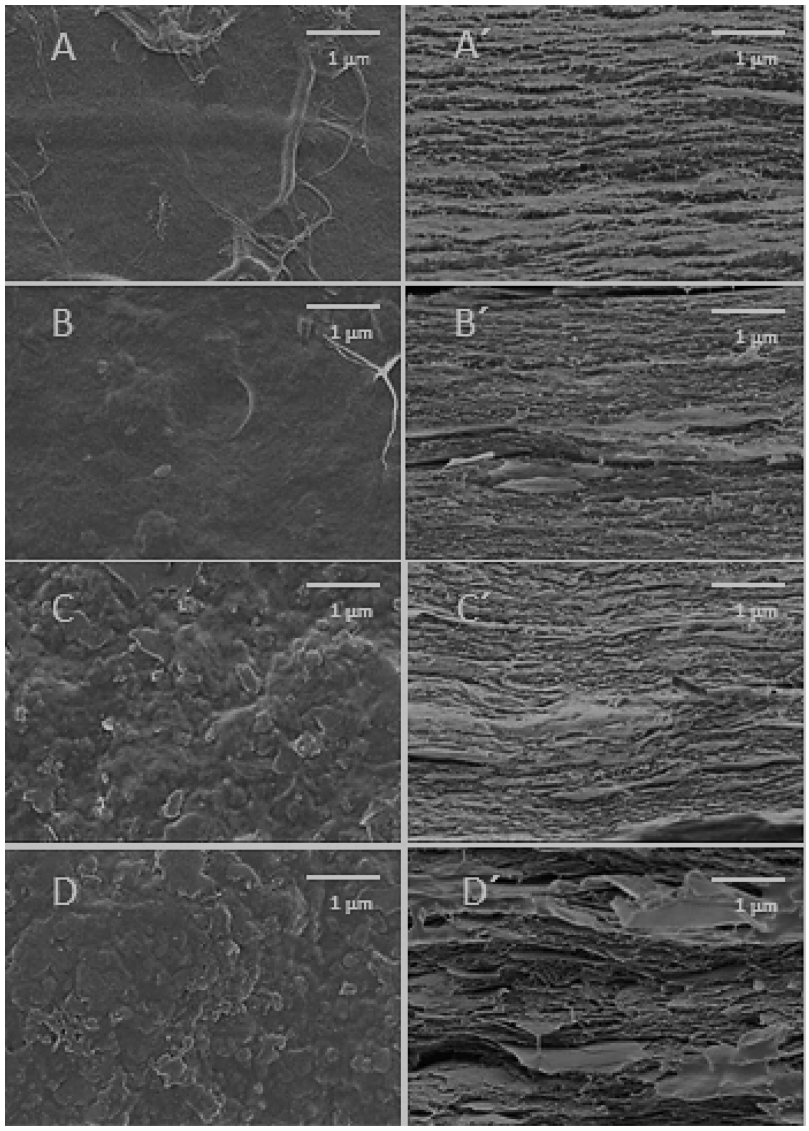

Figure 2. FESEM images of DCC−talc hybrid films in planar (left) and cross-sectional (right) directions: DCC99-Talc1 (A and A′), DCC90-Talc10 (B and B′), DCC75-Talc25 (C and C′), and DCC50-Talc50 (D and D′).

static interaction between nanofibers and talc was probably weak due to the low charge density of talc.

Mechanical and Optical Properties of Hybrids. All DCC−talc hybrid films were flexible in bending and varied visually from highly transparent to fully opaque with a white color (Figure 3A). The optical transmittance of hybrids at 550 nm decreased almost linearly from the pure DCC film's initial value of approximately 90−20% as the talc content increased to 50% (Figure 3B). These transmittance values were comparable to those previously reported for NFC−TiO_2[13] and NFC−montmorillonite[10] hybrids, although the film thicknesses were significantly higher in our case (approximately 6 vs 40 μm, Table 1). As earlier described, the small changes in curvature as a function of mineral content may indicate some level of aggregation of particles, which increased both reflectivity and surface roughness of the hybrids.[13]

The stress−strain curves of DCC−talc hybrid films are presented in Figure 4. The pure DCC nanofiber film showed high tensile strength and Young's modulus values (211 MPa and 12.0 GPa, respectively), indicating that the nanofibers maintained their good strength properties after oxidative pretreatment and homogenization. These values are comparable to those earlier reported for carboxymethylated[5] and TEMPO-oxidized[10,26] NFC films and are higher than those for some other NFC films[27] and many synthetic polymeric films, such as polyethylene terephthalate (PET), polystyrene, and low-density polyethylene (LDPE).[28]

The strain to failure remained at an almost constant value of approximately 5% for all talc-containing hybrid structures. Apparently, the presence of some larger-diameter nanofibers in the present NFC somewhat decreases strain to failure, compared to carboxymethylated NFC,[25] whereas the strength was comparable. Ultimate tensile strength and modulus obtained from the stress−strain curves decreased almost linearly as a function of talc content (Figure 5). However, the values obtained at the highest talc content of 50% were still twice of those previously reported for cationic NFC−talc films[15] (135 vs 67 MPa, and 9.4 vs 4.7 GPa, respectively) and also higher than those for NFC−montmorillonite hybrids[11] (135 vs 124 MPa, and 9.4 vs 8.7 GPa, respectively). Similar strength values have been obtained for natural biohybrids such as nacre.[29] The improvement in the mechanical properties of

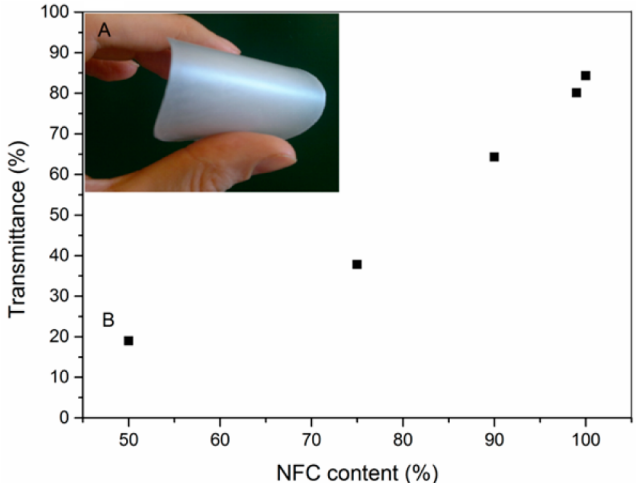

Figure 3. Appearance of DCC–talc films. (A) A photograph of a DCC50-Talc50 hybrid film. (B) Light transmittance of hybrid films at 550 nm as a function of NFC content. Film thicknesses are presented in Table 1.

Table 1. Volume Fraction, Porosity, Density, and Thickness of DCC–Talc Hybrid Films

sample	volume fraction of DCC/talc (%)	porosity (%)	density (g/cm^3)	thickness (μm)
DCC100	100/0	24.4	1.47	40
DCC99-Talc1	99/1	23.6	1.47	48
DCC90-Talc10	93/7	21.0	1.50	47
DCC75-Talc25	82/18	19.7	1.63	39
DCC50-Talc50	62/38	15.6	1.78	38

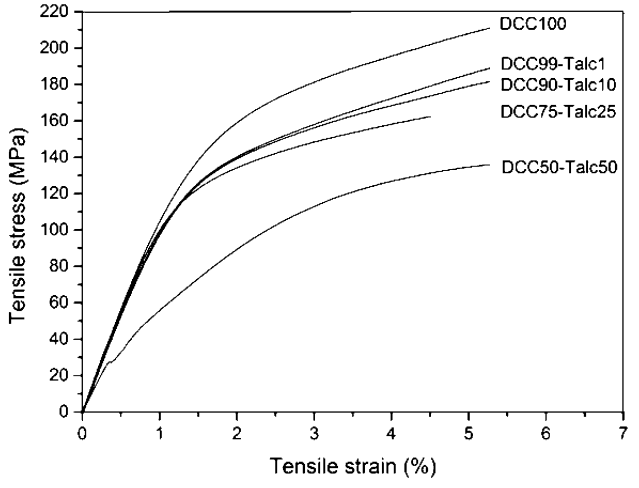

Figure 4. Tensile stress–strain curves of DCC–talc hybrid films. The numbers in the material designations refer to weight percent of each component; see Table 1.

talc hybrids, compared to previously reported results, was probably because of a more efficient disintegration process used to break down the talc platelet aggregates. Talc aggregates are likely to be sites for fracture initiation and thus lead to reduced tensile strength.

The main load-carrying component of hybrids was the NFC network, which probably redistributes stress around inorganic stress concentration sites.[11] Decrease in ultimate tensile strength as a function of talc platelet content indicated that the interaction and load transfer between the DCC nanofiber

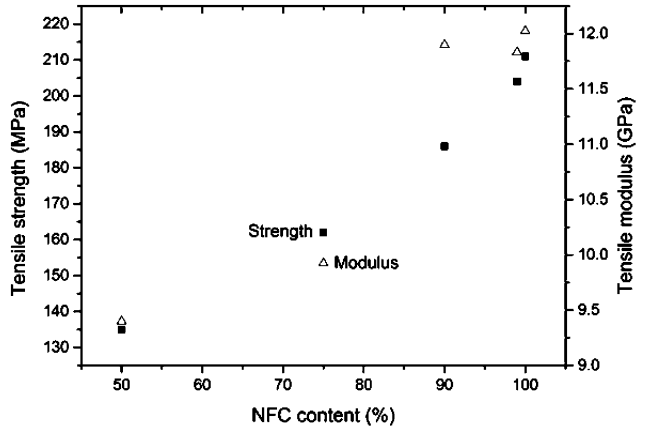

Figure 5. Tensile strength and modulus of DCC–talc hybrid films as a function of nanofiber content.

network and talc platelets were not optimized. This phenomenon was due to anionic carboxylic acid functionalities of DCC nanofibers that repelled negatively charged talc platelets. Consequently, higher strength properties may be achieved, e.g., by using compatibilizers. As an example, chitosan has been used to promote interaction in NFC–montmorillonite hybrids.[12] In addition, a more ordered arrangement of talc platelets in the planar direction similar to the nacre structure could increase mechanical properties of hybrids.

Table 1 shows the porosities of DCC–talc hybrids, as determined by helium gas pycnometry. As already indicated from the cross-sectional FESEM images, the porosities of films decreased as a function of talc content. This phenomenon, together with the increase in hybrid density with higher talc content, indicated that the talc platelets were tightly embedded in the DCC nanofiber network. The presence of nanoscale pores may be of interest for the fabrication of nanoporous structures, e.g., for biosensing purposes.[30]

Surface Properties of Hybrids. The surface characteristics of hybrid films were evaluated in terms of water contact angles. The contact angles of all tested films were below 50°, indicating the hydrophilic nature of the films (Table 2). These values are

Table 2. Contact Angles of DCC–Talc Hybrid Films and Talc Material

sample	contact angle (deg)
DCC100	42 ± 4
DCC99-Talc1	40 ± 2
DCC90-Talc10	45 ± 4
DCC75-Talc25	49 ± 4
talc	75 ± 2

similar to those previously reported for TEMPO-oxidized NFC films.[31] The contact angle values increased slightly as a function of talc content, probably because of talc hydrophobicity (Table 2) and increased film surface roughness.[31] However, the hydrophilicity of anionically charged nanofibers was still the major factor determining the surface characteristics of the films.

Water Vapor Adsorption and Oxygen Barrier Properties. As expected, the moisture uptake of hybrids was significantly decreased from the initial value of approximately 9% to 4% at the highest talc content (Figure 6). The data scale with cellulose content was as expected, since hydrophobic talc is unlikely to adsorb moisture. At 75 wt % NFC, the moisture

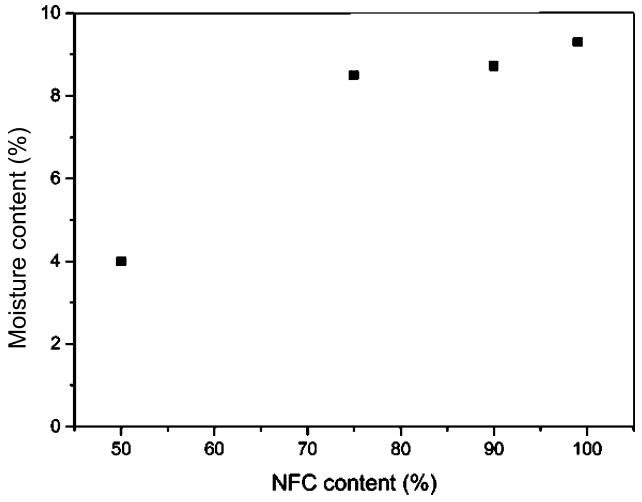

Figure 6. Moisture content of DCC–talc hybrid films as a function of nanofiber content at 80% relative humidity and 20 °C temperature.

content was unexpectedly high. The reason may be in the details of the porous NFC network structure, for instance, increased specific surface area, compared with the 100% NFC reference.

To evaluate gas-barrier properties of DCC–talc hybrids, a preliminary test of oxygen transmission was conducted for the DCC75-Talc25 sample at 50% relative humidity. The OTR of the sample was below the detection limit of the equipment, i.e., less than 0.001 cm^3 mm/m^2 day atm, indicating that the layered structure of hybrids effectively restricted gas diffusion through the film and showing that the DCC–talc hybrid had better barrier properties than those of many synthetic polymers.[5]

CONCLUSIONS

The NFC–talc hybrid films with a lamellar brick-and-mortar structure were fabricated from cellulose nanofibers obtained from sequential periodate–chlorite oxidation and talc platelets using a vacuum-filtration method. To promote homogeneity of hybrid structures, commercial talc aggregates were disintegrated before film formation into well-dispersed individual platelets, using a wet stirred media mill with high-shear conditions. The nanofiber–talc hybrids, which had talc contents from 1 to 50 wt %, were all flexible in bending and possessed tensile strength and Young's modulus values up to 211 ± 3 MPa and 12 ± 1 GPa, respectively—substantially higher than those previously reported for NFC–talc films. The obtained improvement in the mechanical properties of talc hybrids was caused by the efficient disintegration process used to break down the talc platelet aggregates. The individual platelets were then evenly distributed and tightly embedded in the NFC network, which also resulted in the low pore size of the films and good oxygen-barrier properties. The addition of talc platelets decreased the moisture adsorption of highly talc-loaded hybrids, which was roughly proportional to the decreased weight fraction of the NFC.

ASSOCIATED CONTENT

Supporting Information

Sequential periodate–chlorite oxidation pretreatment and appearance of oxidized cellulose before and after homogenization. This material is available free of charge via the Internet at http://pubs.acs.org.

AUTHOR INFORMATION

Corresponding Author

*E-mail: Henrikki.Liimatainen@oulu.fi.

Notes

The authors declare no competing financial interest.

ACKNOWLEDGMENTS

This work was financed by The Academy of Finland (Postdoctoral project No. 250940).

REFERENCES

(1) Jackson, A. P.; Vincent, J. F. V.; Turner, R. M. *Proc. R. Soc. B* **1988**, *234*, 415–440.
(2) Meyers, M. A.; Chen, P. Y.; Lin, A. Y. M.; Seki, Y. *Prog. Mater. Sci.* **2008**, *53*, 1–206.
(3) Espinosa, H. D.; Rim, J. E.; Barthelat, F.; Buehler, M. *Prog. Mater. Sci.* **2009**, *54*, 1059–1100.
(4) Sehaqui, H.; Berglund, L. A.; Zhou, Q. *Biomacromolecules* **2011**, *12*, 3638–3644.
(5) Aulin, C.; Salazar-Alvarez, G.; Lindström, T. *Nanoscale* **2012**, *4*, 6622–6628.
(6) Ridgway, C. J.; Gane, P. A. C. *Cellulose* **2012**, *19*, 547–560.
(7) Nogi, M.; Iwamoto, S.; Nakagaito, A. N.; Yano, H. *Adv. Mater.* **2009**, *21*, 1595–1598.
(8) Torvinen, K.; Sievänen, J.; Hjelt, T.; Hellén, E. *Cellulose* **2012**, *19*, 821–829.
(9) Penttilä, A.; Sievänen, J.; Torvinen, K.; Ojanperä, K.; Ketoja, J. A. *Cellulose* **2012**, *20*, 1413–1424.
(10) Wu, C. N.; Saito, T.; Fujisawa, S.; Fukuzumi, H.; Isogai, A. *Biomacromolecules* **2012**, *13*, 1927–1932.
(11) Liu, A.; Walther, A.; Ikkala, O.; Belova, L.; Berglund, L. A. *Biomacromolecules* **2011**, *12*, 633–641.
(12) Liu, A.; Berglund, L. A. *Carbohydr. Polym.* **2012**, *87*, 53–60.
(13) Schütz, C.; Sort, J.; Bacsik, Z.; Oliynyk, V.; Pellicer, E.; Fall, A.; Wågberg, L.; Berglund, L.; Bergström, L.; Salazar-Alvarez, G. *PLoS One* **2012**, *7*, e45828.
(14) Ho, T. T. T.; Ko, Y.S.; Zimmermann, T.; Geiger, T.; Caseri, W. *J. Mater. Sci.* **2012**, *47*, 4370–4382.
(15) Ho, T.T.T.; Zimmermann, T.; Ohr, S.; Caseri, W.R. *ACS Appl. Mater. Interfaces* **2012**, *4*, 4832–4840.
(16) Liu, A.; Berglund, L. A. *Eur. Polym. J.* **2013**, *49*, 940–949.
(17) Krogerus, B. In *Papermaking Science and Technology: Papermaking Chemistry*; Neimo, L., Ed.; Fapet Oy: Helsinki, 1999; p 124.
(18) Aulin, C.; Gällstedt, M.; Lindström, T. *Cellulose* **2010**, *17*, 559–574.
(19) Liimatainen, H.; Visanko, M.; Sirviö, J. A.; Hormi, O. E. O.; Niinimäki, J. *Biomacromolecules* **2012**, *13*, 1592–1597.
(20) Katz, S.; Beatson, R. P.; Scallan, A. M. *Sven. Papperstidn.* **1984**, *65*, 795–816.
(21) Rattaz, A.; Mishra, S. P.; Chabot, B.; Daneault, C. *Cellulose* **2011**, *18*, 585–593.
(22) Sehaqui, H.; Liu, A.; Zhou, Q.; Berglund, L. *Biomacromolecules* **2010**, *11*, 2195–2198.
(23) Palacio, L.; Prádanos, P.; Calvo, J. I.; Hernández, A. *Thin Solid Films* **1999**, *348*, 22–29.
(24) Kogel, J. E., Trivedi, N. C., Barker, J. M., Krukowski, S. T., Eds. *Industrial Minerals and Rocks: Commodities, Markets, and Uses*, 7th ed.; Society for Mining, Metallurgy, and Exploration: Littleton, CO, 2006; p 391.
(25) Sellinger, A.; Weiss, P. M.; Nguyen, A.; Lu, Y. F.; Assink, R. A.; Gong, W. L.; Brinker, C. J. *Nature* **1998**, *394*, 256–260.
(26) Fukuzumi, H.; Saito, T.; Iwata, T.; Kumamoto, Y.; Isogai, A. *Biomacromolecules* **2009**, *10*, 162–165.
(27) Henriksson, M.; Berglund, L.A.; Isaksson, P.; Lindström, T.; Nishino, T. *Biomacromolecules* **2008**, *9*, 1579–1585.
(28) Briston, J. H. *Plastic Films*; John Wiley and Sons Inc: New York, 1988.

(29) Wang, R. Z.; Suo, Z.; Evans, A. G.; Yao, N.; Aksay, I. A. *J. Mater.Res.* **2001**, *16*, 2485−2493.
(30) Mo, Y.; Fei, T. *Nano LIFE* **2012**, *2*, 1230003.
(31) Rodionova, G.; Eriksen, Ø; Gregersen, Ø. *Cellulose* **2012**, *19*, 1115−1123.